



THE UNIVERSITY *of* EDINBURGH

Edinburgh Research Explorer

Common and Distinctive Functions of the Hippo Effectors Taz and Yap in Skeletal Muscle Stem Cell Function

Citation for published version:

Sun, C, De Mello, V, Mohamed, A, Ortuste Quiroga, HP, Garcia-Munoz, A, Al Bloshi, A, Tremblay, AM, Von Kriegsheim, A, Collie-Duguid, E, Vargesson, N, Matallanas, D, Wackerhage, H & Zammit, PS 2017, 'Common and Distinctive Functions of the Hippo Effectors Taz and Yap in Skeletal Muscle Stem Cell Function', *Stem Cells*. <https://doi.org/10.1002/stem.2652>

Digital Object Identifier (DOI):

[10.1002/stem.2652](https://doi.org/10.1002/stem.2652)

Link:

[Link to publication record in Edinburgh Research Explorer](#)

Document Version:

Publisher's PDF, also known as Version of record

Published In:

Stem Cells

General rights

Copyright for the publications made accessible via the Edinburgh Research Explorer is retained by the author(s) and / or other copyright owners and it is a condition of accessing these publications that users recognise and abide by the legal requirements associated with these rights.

Take down policy

The University of Edinburgh has made every reasonable effort to ensure that Edinburgh Research Explorer content complies with UK legislation. If you believe that the public display of this file breaches copyright please contact openaccess@ed.ac.uk providing details, and we will remove access to the work immediately and investigate your claim.



¹ King's College London, Randall Division of Cell and Molecular Biophysics, London, SE1 1UL, UK.; ² University of Aberdeen, School of Medicine, Medical Sciences and Nutrition, Foresterhill, Aberdeen, AB25 2ZD, Scotland.; ³ Systems Biology Ireland; Conway Institute; Belfield; Dublin 4; Ireland.; ⁴ Stem Cell Program, Children's Hospital, Boston, MA 02115, USA; Department of Stem Cell and Regenerative Biology, Harvard University, Cambridge, MA 02138, USA; Harvard Stem Cell Institute, Cambridge, MA 02138, USA.; ⁵ University of Aberdeen, Centre for Genome Enabled Biology and Medicine, School of Medicine, Medical Sciences and Nutrition, Foresterhill, Aberdeen, AB25 2ZD, Scotland.


* Corresponding author: Peter Zammit, King's College London, Randall Division of Cell and Molecular Biophysics, London, SE1 1UL, UK, +44 207 848 6425, peter.zammit@kcl.ac.uk; ⁶ Current address: Technical University of Munich. Faculty of Sport and Health Sciences. Georg-Brauchle-Ring 60, 80992 Munich, Germany; This study was funded by the Medical Research Council grant number (G11001931) awarded to HW and PSZ and BIODESIGN (262948-2) from EU FP7, with additional support from Association Française Contre les Myopathies, Sarcoma UK and the Friends of Anchor.

Received June 14, 2016; accepted for publication January 07, 2017; available online without subscription through the open access option.

©AlphaMed Press
1066-5099/2017/\$30.00/0

This article has been accepted for publication and undergone full peer review but has not been through the copyediting, typesetting, pagination and proofreading process which may lead to differences between this version and the Version of Record. Please cite this article as doi: 10.1002/stem.2652

Common and Distinctive Functions of the Hippo Effectors Taz and Yap in Skeletal Muscle Stem Cell Function

CONGSHAN SUN¹, VANESSA DE MELLO², ABDALLA MOHAMED², HUASCAR P. ORTUSTE QUIROGA¹, AMAYA GARCIA-MUNOZ³, ABDULLAH AL BLOSHI²; ANNIE. M TREMBLAY⁴, ALEXANDER VON KRIEGSHEIM³, ELAINA COLLIE-DUGUID⁵, NEIL VARGESSON², DAVID MATALLANAS³, HENNING WACKERHAGE^{2,6} AND PETER S. ZAMMIT^{1,*} 

Key words. Taz • Yap • Tead • satellite cells • muscle stem cells

ABSTRACT

Hippo pathway downstream effectors Yap and Taz play key roles in cell proliferation and regeneration, regulating gene expression especially via Tead transcription factors. To investigate their role in skeletal muscle stem cells, we analysed Taz *in vivo* and *ex vivo* in comparison to Yap. siRNA knockdown or retroviral-mediated expression of wildtype human or constitutively active TAZ mutants in satellite cells showed that TAZ promoted proliferation, a function shared with YAP. However, at later stages of myogenesis, TAZ also enhanced myogenic differentiation of myoblasts, whereas YAP inhibits such differentiation. Functionally, while muscle growth was mildly affected in Taz (gene *Wwtr1*^{-/-}) knockout mice, there were no overt effects on regeneration. Conversely, conditional knockout of Yap in satellite cells of *Pax7*^{Cre-ERT2/+}; *Yap*^{flox/flox}; *Rosa26*^{LacZ} mice produced a marked regeneration deficit. To identify potential mechanisms, microarray analysis showed many common TAZ/YAP target genes, but TAZ also regulates some genes independently of YAP, including myogenic genes such as *Pax7*, *Myf5* and *Myod1* (ArrayExpress - E-MTAB-5395). Proteomic analysis revealed many novel binding partners of TAZ/YAP in myogenic cells, but TAZ also interacts with proteins distinct from YAP that are often involved in myogenesis and aspects of cytoskeleton organization (ProteomeXchange - PXD005751). Neither TAZ nor YAP bind members of the Wnt destruction complex but both regulated expression of Wnt and Wnt-cross talking genes with known roles in myogenesis. Finally, TAZ operates through Tead4 to enhance myogenic differentiation. In summary, Taz and Yap have overlapping functions in promoting myoblast proliferation but Taz then switches to enhance myogenic differentiation. *STEM CELLS* 2017; 00:000–000

SIGNIFICANCE STATEMENT:

Hippo pathway effectors Yap and Taz play key roles in cell proliferation and tissue growth. We analysed Taz in comparison to Yap in muscle stem cells. Taz promoted proliferation, a function shared with Yap. However, Taz also enhanced differentiation into myotubes, unlike Yap. Muscle growth was af-

ected in Taz (*Wwtr1*^{-/-}) knockout mice, while knockout of Yap produced a clear regeneration deficit. Taz regulates some genes independently of Yap, and Taz also in-

teracts with proteins distinct from Yap, mainly involved in myogenesis/cytoskeleton. In particular, Taz operates through Tead4 to enhance differentiation. In summary, Taz and Yap have overlapping functions in promoting myoblast proliferation but later, Taz also enhances myogenic differentiation.

INTRODUCTION

Transcriptional co-factors Yap (*Yap1*) and Taz (*Wwtr1*) mainly regulate gene expression by binding Tead1-4 transcription factors. Together Yap, Taz and Teads are the nexus of the Hippo signal transduction network that includes the Hippo kinase cascade, comprising kinases Mst1 (*Stk4*), Mst2 (*Stk3*), Lats1 and Lats2 [1-3]. Many other signalling modules also regulate Yap and Taz activity, such as mechanotransduction [4], glucose-signalling [5], GPCR [6], Wnt [7-9], Smad [10, 11], Notch [12], Pten-Akt-mTor [13-16] and Lkb1-Ampk [17-20]. Yap and Taz are inhibited by phosphorylation of multiple HXRSS motifs by Lats1/2, which promotes localisation to the cytosol, 14-3-3 binding and degradation [3, 21]. Yap Ser127 and Taz Ser89 are key phosphorylation sites and mutations at Ser127 or Ser89 to alanine in Yap S127A and Taz S89A prevent phosphorylation at these residues and result in constitutive activity.

Signalling modules involving Yap/Taz control skeletal muscle myogenesis and adaptation to exercise. Tead transcription factors bind CATTCC/GGAATG (MCAT or GTIIC motifs) often found near promoters of cardiac and skeletal muscle genes [3, 22], and by binding enhancers [23, 24]. However, Tead1 binds muscle genes repressed in rhabdomyosarcoma [25], consistent with observation that Yap and Taz can also repress gene expression [26].

Satellite cells are responsible for postnatal skeletal muscle growth, hypertrophy and repair/regeneration [27], and we have shown that Yap promotes proliferation of myoblasts [28, 29] but inhibits myogenic differentiation. YAP1 S127A expression in activated, but not quiescent, satellite cells causes embryonal rhabdomyosarcoma-like tumours with short latency and 100% penetrance [25]. Expression of YAP1 S127A in muscle fibres causes myopathy [30] whereas other types of Yap delivery or Yap mutants can cause hypertrophy [31, 32], with outcome likely dependent on Yap levels.

Taz harbours the same functionally important WW and Tead-binding domains as Yap and often acts as a paralogue, but not always [2, 3]. This is demonstrated by Yap or Taz knockout mice: while Yap knockout causes early embryonic lethality [33], 50% of Taz (*Wwtr1*) knockout mice are viable but develop glomerulocystic kidney disease [34]. Earlier reports suggest that Yap and Taz also have divergent functions in the skeletal muscle lineage: both Yap and Taz promote skeletal muscle fibre hypertrophy and regeneration [35, 36], but only Taz promotes fusion into multinucleated myotubes [29, 37, 38].

The distinct functions of YAP and TAZ are poorly understood, so we investigated their regulation, function,

target genes and binding partners in murine myoblasts. Taz and Yap have overlapping functions in promoting satellite cell proliferation. However, later in myogenesis, Taz enhances myogenic differentiation and fusion, a function not shared by Yap. Taz (*Wwtr1*^{-/-})-null mice had no overt muscle regeneration phenotype, unlike mice with conditional knockout of Yap in satellite cells. To understand mechanism, we examined gene expression, and found for example, that YAP and TAZ both alter expression of multiple Wnt pathway genes. In addition to common targets, TAZ also regulates a separate set of genes from YAP during myogenesis, including myogenic factors *Pax7*, *Myf5* and *MyoD*. Using proteomics to identify binding partners of TAZ and YAP, we discovered both common and distinct interactors, with TAZ binding proteins that regulate myogenesis and aspects of cytoskeleton organization. Finally, we found that TAZ operates through Tead4 in myoblasts to enhance myogenic differentiation.

MATERIALS AND METHODS

Animals

Taz (*Wwtr1*)-knockout (Jax, stock 011120) and *Yap*^{fl/fl} mice are described [39, 40]. *Pax7*^{Cre} mice were purchased from Jax (stock 012476). *Pax7*^{Cre}:*Yap*^{fl/fl}:*R26-floxstop-LacZ* [9] mice were donated by Fernando Cargano. Breeding/experimental procedures were approved by the Ethical Review Process Committee of KCL, and performed under the Animals (Scientific Procedures) Act 1986.

Cell culture

Satellite cells/myofibres were isolated as described previously [41]. Briefly, murine extensor digitorum longus (EDL) myofibres were isolated by 0.05% type I collagenase for 2h. Myofibres were washed in GlutaMax DMEM (ThermoFisher Scientific) and plated on matrigel-coated plates in growth medium (GlutaMax DMEM, 30% foetal bovine serum (FBS), 1% chick embryo extract (CEE), 10ng/ml basic fibroblast growth factor, 1% penicillin-streptomycin) at 37°C with 5% CO₂. After 72h, myofibres were removed, and satellite cells passaged and pre-plated for 30 min to remove fibroblasts, before being plated on matrigel-coated plates. Differentiation was induced in differentiation medium (GlutaMax DMEM, 2% horse serum, 1% penicillin-streptomycin). Non-adherent cultures: myofibres were cultured in GlutaMax DMEM, 10% horse serum, 0.5% CEE, 1% penicillin-streptomycin.

Muscle injury

To recombine via *loxP* sites flanking *Yap* exons 1 and 2, 200µg of Tamoxifen/gram body weight (Sigma T5648) was injected intraperitoneally in sunflower oil/5% ethanol for 3 consecutive days, followed by maintenance on a tamoxifen-containing diet (Tekland). Injury was induced in tibialis anterior (TA) by 30µl intramuscular injection of 20µM cardiotoxin/saline.

Retroviral expression and siRNA

Wildtype TAZ, TAZ S89A, YAP S127A or wildtype YAP was subcloned into a pMSCV-IRES-eGFP retroviral expression backbone (Addgene Plasmids 24809, 24815, 17791 and 17790) creating pMSCV-3xFlag TAZ-IRES-eGFP and pMSCV-3xFlag-TAZ S89A-IRES-eGFP [42]. Empty vector was negative control. Retroviruses were packaged in HEK293T cells using standard methods. Medium was changed 1h before transfection/transduction. Retroviral suspension diluted 1:4 with Polybrene (4µg/ml) was added for 6h, before changing medium.

Taz siRNA (Ambion, s97145) and Yap siRNA (Ambion, s202423) were used as per manufacturer's instructions. For plated satellite cells, 25 pmol of siRNA with Lipofectamine RNAiMax (ThermoFisher Scientific) was added to each well for either 6h (satellite cells) or 24h (C2C12) before medium was changed.

RT-qPCR

Total RNA was extracted with RNeasy (Qiagen) and reverse transcribed using QuantiTect reverse transcription (Qiagen) as per manufacturer's instructions. RT-qPCR was performed with Brilliant II SYBR green reagents and a ROX reference dye (Stratagene) using the ViiA7 qPCR system. Primer sequences were Yap (5'-TGAGCCCAAGTCCCACTC-3'; R-5'-TGTGAGTGTCCAGGAGAAA-3'), Taz (5'-TATCCAGCCAAATCTCGTG-3'; R-5'-TTCTGCTGGCTCAGGGTACT-3') or as described [43].

Immunolabelling and EdU pulsing

Cells/myofibres were fixed with 4% paraformaldehyde (PFA)/PBS for 10 min, permeabilised with 0.5% Triton-X100/PBS and blocked with 10% Goat serum/PBS or 0.035% carrageenan/PBS followed by incubation with antibodies overnight at 4°C [41]. Antibodies: anti-Pax7 (DSHB); anti-MyHC (MF20, DSHB); anti-myogenin (F5D, DSHB); anti-MyoD (clone 5.8A, DakoCytomation); anti-Taz (HPA007415, Sigma); anti-Yap1 (2F12, Abnova); anti-Tead4 (M01, Abnova).

Cryosections were fixed with 4% PFA/PBS followed by cooled methanol before antigen retrieval in heated citrate buffer [44] and blocking in 10% Goat Serum/PBS. Antibodies: anti-MyHC Type I (BA-D5, DSHB), anti-MyHC Type IIa (A4.74, DSHB) and anti-laminin (Sigma, L9393). Fluorochrome-conjugated secondary antibodies were from ThermoFisher Scientific.

10µM 5-ethyl-2'-deoxyuridine (EdU) was added for 2h before fixation and incorporation detected using Click-iT (ThermoFisher Scientific) according to manufacturer's instructions.

Western blotting

Western blotting was performed using Run Blue precast native Page gels (Expedeon). Protein transfer was performed with the XCell II blot module (ThermoFisher Scientific). PVDF membranes were incubated with antibodies overnight/4°C and visualized using fluorochrome-conjugated secondary antibodies (ThermoFisher Scientific) and digitally imaged.

Mass Spectrometry

C2C12 cells were grown in DMEM (D5761) with 10% FBS and 4mM glutamine. Proliferating C2C12 cells were at 50% cell density. Confluent cultures were differentiated for 72h in DMEM, 2% horse serum, 4mM glutamine.

For immunoprecipitation, 80,000 C2C12s were seeded per 10cm dish. The following day, fresh medium was added 1h prior to addition of 1:5 diluted TAZ or YAP encoding retroviral supernatant. The next day, cells were re-plated and transduction confirmed by GFP. Cells were washed on ice with PBS, and collected in lysis buffer (150mM NaCl, 20mM Tris-HCl pH 7.5, 1% Triton x100) with 1mM sodium orthovanadate, protease inhibitor cocktail (Sigma, p8340) and PMSF. Lysates were incubated for 1h on ice and centrifuged at 14,000 RPM at 4°C for 5 min and supernatant incubated at 4°C with anti-Flag M2 agarose beads (Sigma). Beads were washed three times with washing buffer (150mM NaCl; 20mM Tris-HCL pH 7.5). Sample preparation/mass spectrometry were as described [45], with proteomics data deposited to the ProteomeXchange Consortium via the PRIDE [46] partner repository: identifier PXD005751.

Microarray

Total RNA was isolated from TAZ S89A or YAP S127A transduced myoblasts after 24h or 48h using TRIzol (ThermoFisher Scientific) followed by purification and DNase digestion (RNeasy minikits, Qiagen). RNA quantification was performed on a Nanodrop spectrophotometer (ThermoFisher Scientific) and quality tested on an Agilent TapeStation (RIN 7.6-9.8). Generation of sense strand cDNA, second strand synthesis, in vitro transcription cRNA synthesis, single stranded cDNA synthesis and RNA hydrolysis, fragmentation and labelling were as manufacturer's instructions (GeneChip WT Plus reagent kit, Affymetrix). Hybridisation, washing, staining and scanning of microarrays were carried out on Affymetrix Mouse Gene 2.0 ST microarrays using a GeneChip Fluidics station 450 and GCS3000 scanner (Affymetrix®).

Data pre-processing/quality control was performed using Affymetrix® Genechip® Expression Console v1.2. Probe cell intensity data (CEL files) were processed using the RMA16 algorithm (Affymetrix), which fits a linear model at probe level by employing background cor-

rection, quantile normalisation of log₂ transformed data and summarisation, for primary QC analysis. Performed in triplicate at Centre for Genome Enabled Biology and Medicine (University of Aberdeen).

Data analysed in Partek® Genomics Suite®, version 6.6, build 6.15.0730 Copyright ©; 2014 (Partek Inc.) using a Mouse Gene 2.0 ST annotation file from build mm10, MoGene-2.0-st-v1.na35.mm10.transcript. Affymetrix CEL files were imported to Partek® Genomics Suite®, data processed using RMA normalisation with RMA background correction and quantile normalisation of log₂ transformed data and probeset summarisation by median polish. 2-way Analysis of Variance with time point (24h, 48h) and transcription factor (Control, TAZ S89A, YAP S127A) and time*transcription interaction to evaluate significantly differentially expressed genes. Fold change of TAZ S89A or YAP S127A compared to control vector as baseline at each time point calculated using geometric mean of samples in each group with significance calculated by Fishers Least significant difference. Fold change ≥ 1.3 and FDR of 10% were evaluated. Microarray data available in the ArrayExpress database (www.ebi.ac.uk/arrayexpress), accession number E-MTAB-5395.

Histology

Haematoxylin & Eosin and ATPase staining were described previously [30]. Muscle sections were stained with ATPase at pH 4.47 to detect type I, and pH 10.5 to detect type II, myofibres.

Image Acquisition and analysis

Images were obtained at room temperature on a Zeiss microscope (Axiovert 200M) equipped with LD A-plan 20x/0.85 ph1, 10x/0.30ph1 and 40x/.075ph1 objectives or on a Zeiss Exciter laser scanning microscope (LSM) with 40x/1.1 W Corr LD C-Apochromat objective. Images were quantified with image J software (NIH, USA). Neonatal MyHC labelling was quantified with R software. Values are mean \pm SEM with a Student's *t*-test (paired or unpaired as appropriate) or ANOVA with a post-hoc Tukey's test for >2 groups.

RESULTS

Taz is dynamically regulated during myogenic progression

To assess *Yap* and *Taz* expression dynamics during muscle regeneration, we measured mRNA levels by RT-qPCR in vivo and myogenic progression in vitro. Murine TA muscle was injured by intramuscular injection of cardiotoxin and mRNA isolated from regenerating muscle after 1, 3, 5, 7 and 14 days post-injury (dpi). *Taz* mRNA increased markedly at 3 dpi compared to uninjured control, before dropping, while *Yap* was largely unchanged (Figure 1A). *Taz* mRNA rose during differentiation of C2C12 myoblasts, while *Yap* mRNA remained relatively constant (Figure 1B). Western blot analysis for total Yap

and Taz protein in C2C12 reflected mRNA dynamics, with Taz levels rising during differentiation, while Yap again remained relatively constant (Figure 1C). Phosphorylated Yap and Taz levels both showed an increase during myogenic differentiation. *Taz* mRNA also increased during ex-vivo differentiation of plated murine satellite cell-derived myoblasts (Figure 1D).

Co-immunolabelling C2C12 myoblasts for Yap and Taz revealed Taz localised to the cytoplasm and nucleus, while Yap was nuclear (Figure 1E), consistent with our previous observations [29]. Taz was similarly localised in satellite cells (Figure 1F), but became cytoplasmic in mature multinucleated myotubes (Figure 1G). Co-immunolabelling of satellite cells in their niche on a myofibre showed that Taz was expressed in satellite cells as shown by MyoD co-expression (Figure 1H).

Taz promotes myoblast proliferation

To compare Taz with Yap function, we either increased Taz activity via retroviral-mediated expression of human TAZ or constitutively active TAZ S89A, or after decreasing Taz and/or Yap levels using siRNA and performed proliferation and differentiation assays.

The retroviral backbone contains an *IRES-eGFP* that allows transduced cells to be identified by eGFP. Immunolabelling revealed that TAZ or TAZ S89A significantly increased the proportion of eGFP+ve cells that had incorporated EdU, indicating that TAZ increases proliferation (Figure 2A,B). siRNA-knockdown of *Taz*, *Yap* or both *Taz/Yap* however, significantly reduced EdU incorporation (Figure 2C,D). Thus at this stage, TAZ promotes proliferation of myoblasts, as we previously reported for YAP [28, 29].

RT-qPCR showed that siRNA-mediated knockdown of *Taz* suppressed *Myf5* and *myogenin* expression, but enhanced *Pax7*. Conversely, knockdown of Yap increased *myogenin* expression, but reduced *Pax7* and *Myf5*. Simultaneous knockdown of both *Taz* and *Yap* rescued expression of *myogenin* (Figure 2E).

Taz and Yap play opposing roles during myogenic differentiation

We determined the effect of retroviral-mediated constitutive expression of TAZ or TAZ S89A on early myogenic differentiation in satellite cells cultured in their niche for 72 hours on an isolated myofibre, by co-immunolabelling for eGFP/Pax7 to mark undifferentiated/self-renewing cells (Figure 3A) or eGFP/myogenin to mark myoblasts entering differentiation (Figure 3B). TAZ significantly decreased eGFP-containing self-renewing Pax7+ve cells (Figure 3A), while TAZ or TAZ S89A significantly increased eGFP-containing differentiating myogenin+ve myoblasts (Figure 3B), compared with control. Thus TAZ promotes entry into differentiation, at the expense of satellite cell self-renewal.

To investigate effects of TAZ or TAZ S89A throughout myogenic differentiation, we used expanded, plated satellite cell-derived myoblasts, which were first trans-

duced and then switched to differentiation medium 24 hours later. Self-renewal and differentiation were again assessed by co-immunofluorescence for eGFP/Pax7 and eGFP/myogenin. Under differentiation stimulus, TAZ or TAZ S89A decreased the proportion of myocytes expressing Pax7, while enhancing the proportion expressing myogenin (Figure 3C,D). At this early stage of differentiation, myotubes were also more prominent in myoblast cultures transduced with TAZ or TAZ S89A, than control retrovirus, suggesting a time-dependent switch of TAZ function from pro-proliferation to pro-differentiation (Figure 3E). At later stages of differentiation and fusion into multinucleated myotubes, constitutive expression of TAZ or TAZ S89A also increased incorporation of nuclei into myotubes (fusion index - Figure 3F,G). siRNA-mediated Taz knockdown in expanded plated satellite cell-derived myoblasts did not significantly reduce (though $p=0.06$) the fusion index to below control levels (Figure 3H,I).

Taz (*Wwtr1*^{-/-})-null myoblasts differentiate less ex vivo

Skeletal muscles of *Taz* (*Wwtr1*^{-/-})-knockout mice have not been well-characterized [40]. Consistent with the trend in siRNA data (Figure 3H,I), satellite cells isolated and expanded from *Taz* (*Wwtr1*^{-/-})-null mice fused less into post-mitotic myotubes compared to wildtype cells (Figure 3J,K).

Thus, Taz promotes proliferation of myoblasts, but at later stages of myogenesis, Taz switches to enhance differentiation, while, as we previously reported, Yap continues to promote proliferation whilst inhibiting differentiation [28, 29].

Taz (*Wwtr1*^{-/-})-null mice have fewer myofibres in Soleus

In accordance with the role of the Hippo pathway in body/organ size regulation, 6-week-old *Taz* (*Wwtr1*^{-/-})-knockout mice were lighter than wildtype mice (Figure 4A) as were their TA, soleus, EDL and gastrocnemius muscles (Figure 4B-E). However, the number of satellite cells and myonuclei per EDL myofibre was unchanged between *Taz* (*Wwtr1*^{-/-})-null and wildtype mice (Figure 4F,G). Myofibre type composition in soleus was analysed using ATPase activity at pH 4.47 to detect slow type I, or pH 10.5 to detect fast type IIa, myofibres. Soleus contained fewer muscle fibres in total, with both numbers of type I and type IIa myofibres significantly reduced compared to wildtype (Figure 4H,I), but the proportion of slow type I myofibres was significantly increased, while the proportion of type IIa were significantly decreased, compared to control wildtype. Myofibre cross-sectional area was unchanged though (Figure 4J).

Next, we investigated muscle regeneration in the *Taz* (*Wwtr1*^{-/-})-knockout mice using intra-muscular injection of cardiotoxin into TA. Cryosections of 5 dpi regenerating TA were immunolabelled for neonatal MyHC

to identify regenerating myofibres, but *Taz* (*Wwtr1*^{-/-})-knockouts did not exhibit a reduction compared to controls (Figure 4K,L). At 10 dpi, the number of myofibres with centrally located nuclei in TA of *Taz* (*Wwtr1*^{-/-})-null mice was also unchanged (Figure 4M,N).

Inactivation of Yap in satellite cells impairs muscle regeneration

Administration of Tamoxifen to *Pax7*^{Cre-ERT2/+}:*Yap*^{flox/flox}:*Rosa26*^{LacZ} mice causes Pax7-driven Cre-ERT2-mediated deletion of *Yap* exons 1 and 2 in satellite cells, with simultaneous induction of *lacZ* expression. *Pax7*^{Cre-ERT2/+}:*Yap*^{flox/flox}:*Rosa26*^{LacZ} and age-matched control *Pax7*^{Cre-ERT2/+}:*Yap*^{flox/+}:*Rosa26*^{LacZ} mice were given three intraperitoneal injections of Tamoxifen, and then maintained on tamoxifen-containing food. TA muscles were injured by intramuscular injection of cardiotoxin, and regenerating muscles cryosectioned at 5 and 10 dpi (Figure 5A).

Regenerating TA muscles at 5 dpi from Tamoxifen-treated *Pax7*^{Cre-ERT2/+}:*Yap*^{flox/flox}:*Rosa26*^{LacZ} mice co-immunolabelled for neonatal MyHC and laminin had a 30% smaller area containing neonatal MyHC than control *Pax7*^{Cre-ERT2/+}:*Yap*^{flox/+}:*Rosa26*^{LacZ} (Figure 5B,C). Immunolabelling for Pax7 revealed that there was a non-significant ($p=0.054$) trend to reduced numbers of satellite cells in Tamoxifen-treated 5 dpi regenerating *Pax7*^{Cre-ERT2/+}:*Yap*^{flox/flox}:*Rosa26*^{LacZ} muscle (Figure 5D,F).

By 10 dpi, Pax7 immunolabelling revealed that satellite cell number in tamoxifen-treated *Pax7*^{Cre-ERT2/+}:*Yap*^{flox/flox}:*Rosa26*^{LacZ} mice was as in control *Pax7*^{Cre-ERT2/+}:*Yap*^{flox/+}:*Rosa26*^{LacZ} mice (Figure 5E,F). The number of myofibres with centrally-located myonuclei, a hallmark of regenerated muscle, was also unchanged between *Pax7*^{Cre-ERT2/+}:*Yap*^{flox/flox}:*Rosa26*^{LacZ} regenerating TA muscles and control (Figure 5G,H). Thus lack of Yap function in satellite cells slows, but does not prevent, muscle regeneration.

YAP and TAZ regulate the Hippo negative feedback loop, myogenic regulators and Wnt signalling

To compare the effects of TAZ and YAP on gene expression in the skeletal muscle lineage, we expressed TAZ S89A or YAP1 S127A in proliferating murine satellite cell-derived myoblasts for 24 and 48 hours and analysed gene expression by microarray (Supplementary data 1), comparing our observations with those obtained by induction of YAP1 S127A in myoblasts derived from a transgenic mouse model [29] and from rhabdomyosarcomas driven by YAP1 S127A [25].

Combination of 24 and 48 hour time points revealed that TAZ S89A significantly changed expression of 860 genes, while YAP S127A altered expression of 294 genes, with an additional 316 genes regulated by both TAZ S89A and YAP S127A (Figure 6A, Supplementary data 1). Satellite cells were already actively proliferating as cultured in high serum medium, and serum is a po-

tent YAP activator [47], likely explaining why neither TAZ S89A nor YAP1 S127A significantly affected most mitotic genes, in contrast to earlier observations [25, 29].

Increased TAZ/YAP-Tead activity was indicated by both TAZ S89A and YAP S127A inducing the Hippo negative feedback loop genes *Amotl2*, *Frmd6* (Willin) and *Lats2*, which was presumably to limit Taz/Yap activity. TAZ S89A and YAP S127A also regulate markers/regulators of the muscle lineage: *Caveolin1* (Cav1) was up-regulated, while *Six1* and *Six4* were down-regulated. In addition, TAZ and YAP regulated multiple members of the mTOR/IGF pathway, including *Igfbp5*, as well as *Ndrp2* and *Irs2*, which regulate mTOR via Akt (Figure 6B).

Wnts are TAZ / YAP regulators, and TAZ / YAP regulation of Wnt and Wnt-related proteins can inhibit Wnt signalling [48]. TAZ S89A and YAP S127A altered expression of key Wnt pathway regulators, reducing expression of Wnt-receptor proteins *Fzd7* and *Lgr5*, while TAZ S89A alone suppressed expression of *Fzd6*, *Lgr4* and *Lgr6*, suggesting that TAZ/YAP desensitize myoblasts to ligands that bind these receptors. Moreover, TAZ S89A increased expression of *Wnt4*, and altered expression of other secreted Wnt-associated proteins and genes encoding the structurally related proteins *Wisp1* and *Wisp2* [49]. Additionally both TAZ S89A and YAP S127A decreased *Sox9* expression (Figure 6B and C).

TAZ regulates a unique set of genes

Although the microarray was performed on proliferating myoblasts, genes regulated by TAZ only might explain the functional switch from pro-proliferation to pro-differentiation (Figure 6C). Both *Pax7* and *MyoD* were down-regulated by TAZ S89A while *Myf5* was up-regulated, consistent with Taz siRNA knockdown (Figure 2E). Up-regulated cell junction proteins could contribute to enhanced fusion capability in TAZ-overexpressing myoblasts, since N-Cadherin is required for myoblast fusion [50]. TAZ overexpression also altered expression of olfactory receptors *Olfr311* and *Olfr1086* (Figure 6C), a family of genes engaged in satellite cell self-renewal [51]. *Mki67* (protein Ki67) involved in proliferation, but was down-regulated by TAZ in myoblasts (Figure 6C), again highlighting the switch from promoting proliferation towards cell cycle withdrawal/differentiation.

YAP and TAZ bind both common and unique proteins

Apart from Tead1-4, Yap and Taz also bind a plethora of upstream signalling proteins and downstream transcriptional regulators [52]. To identify binding partners in a non-biased way, we expressed flag-tagged wildtype human YAP or TAZ in proliferating murine C2C12 myoblasts and mature myotubes. Flag-immunoprecipitated YAP or TAZ complexes were identified using mass-spectrometry (Figure 6D, Supplementary data 2).

Our TAZ and YAP binding proteins were first validated against previously characterised binding partners in human embryonic kidney 293T cells [53]. Overlap included angiomotins, multiple 14-3-3 proteins, Tead1, Tead3, and Tead4 (red: Figure 6D). However, we also identified many novel TAZ and/or YAP interacting proteins in myogenic cells (Figure 6D). TAZ bound many more proteins in myoblasts than YAP, or that were common to both YAP and TAZ. In myotubes however, YAP bound many more proteins than TAZ or both TAZ and YAP, with only YAP binding Wnt regulators *Dvl2* and *Dvl3*. Of 26 TAZ and YAP binding proteins in mature myotubes (Figure 6D), 10 are linked to actin cytoskeleton and the Chaperone assisted selective autophagy (CASA) complex, including the WW-domain containing Bag3. We also identified 20 proteins bound specifically by TAZ during differentiation, the majority associated with the actin cytoskeleton and myogenesis including *Unc45a* and *Fhl3* [54, 55]. *MyoD* was not among YAP and/or TAZ binding partners, even at less stringent cut-offs.

TAZ operates through Tead4 to control myogenic differentiation

We next assayed Tead expression during myogenesis. TA muscle was injured using cardiotoxin and mRNA isolated from regenerating muscle after 1, 3, 5, 7 and 14 dpi. RT-qPCR showed that *Tead2* and *Tead4* exhibited similar expression profiles, peaking around day 3, before falling to levels seen in undamaged muscle (Figure 7A). *Tead1-3* mRNA was at a constant level in proliferating and differentiating C2 myoblasts, but *Tead4* expression increased robustly at the onset of myogenic differentiation, being maintained at elevated levels through fusion (Figure 7B). Western blot revealed that Tead1 and Tead4 protein levels increased upon entry into C2C12 myoblast differentiation, and were maintained (Figure 7C).

As Tead4 is critical for myoblast fusion due to inducing myogenin by binding MCAT elements in its promoter [56], we further examined its function. Co-immunolabelling of Tead4 and Taz showed both proteins present in the nucleus of differentiating myoblasts, at a time when Tead4 levels rise markedly (Figure 7D). Thus the TAZ-Tead4 interaction identified in proliferating myoblasts (but not in mature myotubes) (Figure 6D) could be maintained during induction and the early phases of myogenic differentiation, not assayed by proteomics.

We used retroviral-mediated expression to enhance TAZ activity and/or siRNA to reduce Tead4 levels in satellite cell-derived myoblasts during myogenic differentiation, and assayed fusion index after co-immunolabelling for eGFP/MyHC. TAZ S89A with control siRNA augmented myoblast fusion (Figure 7E,F), but TAZ S89A with concomitant Tead4 knockdown reversed this enhanced fusion index (Figure 7E,F). Knockdown of Tead4 alone resulted in shorter and thinner myotubes, reflected in a reduced fusion index, but expression of

TAZ S89A did allow recover of the fusion index back to control levels (Figure 7E,F).

To investigate the role of TAZ/Tea4 in entry into myogenic differentiation versus fusion, we also transduced satellite cell-derived myoblasts with TAZ S89A and/or transfected with Tea4 siRNA and differentiated cells as myocytes. After 24 hours in differentiation medium, co-immunolabelling revealed that TAZ S89A increased the proportion of eGFP-expressing cells containing myogenin, compared to controls. Knockdown of Tea4 alone significantly reduced myogenin expression (Figure 7G,H). Simultaneous expression of TAZ S89A and Tea4 siRNA knockdown though, brought the proportion of GFP-expressing myoblasts containing myogenin back to control levels (Figure 7G,H).

DISCUSSION

Yap, Taz and Tead1-4 constitute a dynamic system in satellite cells and the muscle lineage, with mRNA and protein levels of some changing extensively during muscle regeneration and myogenic differentiation in vitro. Three are of note: Yap [29] and Taz only become detectable during satellite cell activation, suggesting that Yap and Taz only operate during myogenesis; mRNA/protein levels of some Teads also change, suggesting that Teads are not just static targets of Yap/Taz; Taz and Tead4 increase dramatically during myogenic differentiation, while Yap expression remains fairly constant. During regeneration, Taz and Tead4 levels peak around 3-5 dpi, as myogenic differentiation is underway [57-59]. Our observations are consistent with Taz and Tead4 as pro-differentiation factors [28, 29, 37, 56].

Manipulation of Yap and Taz activity/levels via retroviral-mediated expression of wildtype or TAZ S89A, or knockdown of Taz, revealed that TAZ promotes proliferation. Yap [28, 29] and Taz synergistically promote proliferation in many cell types [60], with a recent ChIP-Seq study in breast cancer cells showing that YAP and TAZ frequently operate through the same enhancer elements [24]. Later in myogenesis however, TAZ switches to promote differentiation, in accordance with an earlier reports in immortalised murine myoblasts [37, 38], unlike YAP, which inhibits differentiation [28, 29]. TAZ actually augments the myogenic differentiation program under differentiation stimuli, as shown by the precocious expression of myogenin in many myocytes. Thus, the greater fusion index with TAZ overexpression is not merely due to having more myoblasts available, due to the pro-proliferation effects of TAZ. Consistent with its later pro-differentiation role, constitutive TAZ expression also reduced self-renewal of satellite cells, while Taz (*Wwtr1*^{-/-})-null satellite cells exhibited reduced fusion ex-vivo.

Taz (*Wwtr1*^{-/-})-null mice have functional and growth defects in kidneys and other organs, consistent with Taz as a regulator of organ growth and transcriptional regulator of genes involved in heart, lung and bone growth [21, 61, 62]. Taz (*Wwtr1*^{-/-})-null mice were generally

lighter, with TA, soleus, EDL and gastrocnemius muscle mass all reduced, but with unchanged numbers of satellite cells and myonuclei per myofibre. However, absence of Taz reduced the total number of myofibres in soleus, with both fewer slow type I and fast Type IIa muscle fibres present, although there was a greater proportion of slow type I myofibres.

Lack of an overt muscle regeneration phenotype in Taz (*Wwtr1*^{-/-})-null mice could be due to compensation by Yap in promoting satellite cell proliferation, as Yap or Taz knockdown did not affect expression of the other gene [63]. In comparison, genetic deletion of Yap specifically in satellite cells caused delayed regeneration, so Taz is unable to compensate for Yap in early regeneration. This regeneration defect in tamoxifen-treated *Pax7*^{Cre-ERT2/+}:*Yap*^{flox/flox}:*Rosa26*^{LacZ} mice was transient though, maybe due to Taz promoting myogenic differentiation later in regeneration. Therefore, skeletal muscle joins other systems where Yap is required for regeneration, for example where defects in crypt regeneration are observed when Yap is inactivated in epithelium of the small intestine, and in the skin [64-66].

We also examined gene expression in myoblasts in response to TAZ S89A or YAP S127A. As expected, YAP and TAZ increased expression of Hippo marker gene *Cyr61* and Hippo negative-feedback loop genes *Lats2*, *Frdm6* (Willin) and *Amotl2*: a typical response to increased Taz and Yap activity [29]. Intriguingly, TAZ also down-regulates *Bag3*, a WW domain-containing member of the CASA mechanosensitive Z-disc linked complex [67] that binds to Yap and Taz, and *Yes1*, the earliest reported binding partner of Yap [68]. *Bag3* and *Yes1* might represent additional members of the Hippo negative feedback loop in myoblasts. Several TAZ- and YAP-regulated genes have been linked to myogenesis. For example, TAZ and YAP reduced expression of *Six1* and *Six4*, two factors controlling migration of muscle precursor cells [69] with a role in muscle regeneration [70]. TAZ and YAP also regulated many IGF/mTOR-related genes (*Ndrq2*, *Igfbp5*, *Irs2* and *Igf2bp1*), confirming cross-talk between Hippo and mTOR signalling [2, 3].

TAZ also regulates a unique cohort of genes, including *Pax7*, whose expression was reduced by TAZ S89A, consistent with the switch towards differentiation. TAZ also modulates multiple olfactory receptor genes, whose levels vary between *mdx* and control mice [51], and a family of genes that can affect muscle regeneration [71].

TAZ and YAP bind proteins in murine myoblasts/myotubes that have been identified as binding partners in human 293T cells [53]. These generic YAP and TAZ binding proteins include the angiopotins (*Amot* and *Amotl1*), *Tead1* and *Tead4* and several 14-3-3 proteins (*Ywhae*, *Ywhag*, *Ywhaz*). Additionally, we identified many novel TAZ and/or YAP binding partners in the skeletal muscle lineage, including in myotubes, *Bag3* [72] and *syncoilin* (*Sync*), an intermediate filament protein linked to the dystrophin-associated protein complex [73]. TAZ-specific binding partners that could

potentially explain pro-differentiation effects include Fhl3, which binds MyoD to inhibit differentiation [55] and Unc45a, which increases muscle cell proliferation and fusion, and when inhibited, blocks muscle cell fusion [54]. Runx1 bound to TAZ in myoblasts and down-regulation of Runx1 leads to cell cycle exit and differentiation [54]. Taz has been reported to bind MyoD using immunoprecipitation assays [37], but while we observed MyoD and Taz in the same nuclei, we found no significant direct interaction using mass spectrometry.

Our combined gene expression and binding partner analyses in myoblasts reveals that YAP or TAZ do not bind members of the Wnt destruction complex [8]. YAP bound the dishevelled proteins Dvl2 and Dvl3 in myotubes, relevant as Dvl2 can affect satellite cell polarity and migration downstream of Wnt7a/Fzd7 [74]. TAZ S89A down-regulates *Fzd6* and *Fzd7*, and *Lgr4*, *Lgr5* and *Lgr6*, important Wnt receptors in developmental and regenerative myogenesis [75, 76], suggesting that TAZ desensitize cells to ligands that bind these receptors. For example, quiescent satellite cells express high levels of *Fzd7* but not Taz or Yap, but during activation, the increased abundance/activity of Yap/Taz could be involved in the down-regulation of *Fzd7*.

Additionally, TAZ S89A increases expression of *Wnt4*, decreases *Sox9* expression and alters expression of secreted Wnt-associated proteins and genes encoding the structurally related proteins *Wisp1*, *Wisp2*, *Igfbp4*, *Cyr61* and *Bmp4* [49]. Many of these genes have been implicated in regulation of developmental myogenesis, satellite cell function and muscle fibres. For example, over-expression of *Wnt4* increased *Pax7* and *MyoD1* expression in chick embryos [77]. *Bmp4* promotes satellite cell proliferation but inhibits differentiation [78].

Interestingly, Tead4 bound TAZ and YAP in proliferating myoblasts but not in mature multinucleated myotubes. Tead4 increases dramatically as myoblasts enter myogenic differentiation and levels are then maintained. Thus the TAZ-Tead4 interaction identified in proliferating myoblasts by proteomics is likely maintained during induction and the early phases of myogenic differentiation, not assayed by proteomics. When Tead4 was knocked-down, myogenic differentiation was suppressed, which recovered to controls levels when TAZ S98A was also expressed. However, TAZ S89A could

no longer enhance entry into the differentiation programme and augment fusion when Tead4 levels were reduced. Thus, the role of TAZ in inducing and promoting myogenic differentiation is linked to interaction with Tead4 [37, 56].

In conclusion, in the skeletal myogenic lineage we demonstrate similar roles of TAZ and YAP in promoting myoblast proliferation, but during the later stages of myogenesis, Taz switches towards influencing satellite cell fate by promoting myogenic differentiation.

ACKNOWLEDGMENTS

CS funded by MRC grant G11001931 to HW and PSZ; CS was also supported by the European Union's Seventh Framework Programme for research, technological development and demonstration under grant agreement number 262948-2 (BIODESIGN); AM, HW and NV supported by Sarcoma UK (award reference: SUK09.2015); VDM was supported by a BBSRC EastBio DTP PhD studentship; with additional support from Association Française Contre les Myopathies, BBSRC, Sarcoma UK and Friends of Anchor.

Authors declare no Potential Conflicts of Interest.

AUTHOR CONTRIBUTIONS

C.S.: Conception and design, Collection and/or assembly of data, Data analysis and interpretation, Manuscript writing; V.D.M.: Collection and/or assembly of data, Data analysis and interpretation; A.M.: Collection and/or assembly of data, Data analysis and interpretation; H.P.O.Q.: Collection and/or assembly of data; A.G.-M.: collection and/or assembly of data; A.A.B.: Collection and/or assembly of data; A.M.T.: Conception and design; A.v.K.: Collection and/or assembly of data, Data analysis and interpretation; E.C.-D.: Collection and/or assembly of data, Data analysis and interpretation; N.V.: Data analysis and interpretation; D.M.: Collection and/or assembly of data, Data analysis and interpretation; H.W.: Conception and design, Data analysis and interpretation, Manuscript writing; P.S.Z.: Conception and design, Data analysis and interpretation, Manuscript writing

REFERENCES

- 1 Harvey K, Tapon N. The Salvador-Warts-Hippo pathway - an emerging tumour-suppressor network. *Nat Rev Cancer*. 2007;7:182-191.
- 2 Hansen CG, Moroishi T, Guan KL. YAP and TAZ: a nexus for Hippo signaling and beyond. *Trends Cell Biol*. 2015;25:499-513.
- 3 Wackerhage H, Del Re DP, Judson RN et al. The Hippo signal transduction network in skeletal and cardiac muscle. *Sci Signal*. 2014;7:re4.
- 4 Dupont S, Morsut L, Aragona M et al. Role of YAP/TAZ in mechanotransduction. *Nature*. 2011;474:179-183.
- 5 Enzo E, Santinon G, Pocaterra A et al. Aerobic glycolysis tunes YAP/TAZ transcriptional activity. *The EMBO journal*. 2015;34:1349-1370.
- 6 Yu FX, Zhao B, Panupinthu N et al. Regulation of the Hippo-YAP pathway by G-protein-coupled receptor signaling. *Cell*. 2012;150:780-791.
- 7 Rosenbluh J, Wang X, Hahn WC. Genomic insights into WNT/beta-catenin signaling. *Trends Pharmacol Sci*. 2014;35:103-109.
- 8 Azzolin L, Panciera T, Soligo S et al. YAP/TAZ incorporation in the beta-catenin destruction complex orchestrates the Wnt response. *Cell*. 2014;158:157-170.
- 9 Xin M, Kim Y, Sutherland LB et al. Regulation of insulin-like growth factor signaling by Yap governs cardiomyocyte proliferation and embryonic heart size. *Sci Signal*. 2011;4:ra70.
- 10 Varelas X, Samavarchi-Tehrani P, Narimatsu M et al. The Crumbs complex couples cell density sensing to Hippo-dependent control of the TGF-beta-SMAD pathway. *Dev Cell*. 2010;19:831-844.

- 11 Alarcon C, Zaromytidou AI, Xi Q et al. Nuclear CDKs drive Smad transcriptional activation and turnover in BMP and TGF-beta pathways. *Cell*. 2009;139:757-769.
- 12 Camargo FD, Gokhale S, Johnnidis JB et al. YAP1 increases organ size and expands undifferentiated progenitor cells. *Curr Biol*. 2007;17:2054-2060.
- 13 Tumaneng K, Russell RC, Guan KL. Organ size control by Hippo and TOR pathways. *Curr Biol*. 2012;22:R368-379.
- 14 Cinar B, Fang PK, Lutchnan M et al. The pro-apoptotic kinase Mst1 and its caspase cleavage products are direct inhibitors of Akt1. *The EMBO journal*. 2007;26:4523-4534.
- 15 Yuan Z, Kim D, Shu S et al. Phosphoinositide 3-kinase/Akt inhibits MST1-mediated pro-apoptotic signaling through phosphorylation of threonine 120. *J Biol Chem*. 2010;285:3815-3824.
- 16 Collak FK, Yagiz K, Luthringer DJ et al. Threonine-120 phosphorylation regulated by phosphoinositide-3-kinase/Akt and mammalian target of rapamycin pathway signaling limits the antitumor activity of mammalian sterile 20-like kinase 1. *J Biol Chem*. 2012;287:23698-23709.
- 17 Nguyen HB, Babcock JT, Wells CD et al. LKB1 tumor suppressor regulates AMP kinase/mTOR-independent cell growth and proliferation via the phosphorylation of Yap. *Oncogene*. 2013;32:4100-4109.
- 18 DeRan M, Yang J, Shen CH et al. Energy stress regulates hippo-YAP signaling involving AMPK-mediated regulation of angiomin-like 1 protein. *Cell Rep*. 2014;9:495-503.
- 19 Wang W, Xiao ZD, Li X et al. AMPK modulates Hippo pathway activity to regulate energy homeostasis. *Nat Cell Biol*. 2015;17:490-499.
- 20 Mo JS, Meng Z, Kim YC et al. Cellular energy stress induces AMPK-mediated regulation of YAP and the Hippo pathway. *Nat Cell Biol*. 2015;17:500-510.
- 21 Kanai F, Marignani PA, Sarbassova D et al. TAZ: a novel transcriptional co-activator regulated by interactions with 14-3-3 and PDZ domain proteins. *The EMBO journal*. 2000;19:6778-6791.
- 22 Mar JH, Ordahl CP. A conserved CATTCT motif is required for skeletal muscle-specific activity of the cardiac troponin T gene promoter. *Proc Natl Acad Sci U S A*. 1988;85:6404-6408.
- 23 Galli GG, Carrara M, Yuan WC et al. YAP Drives Growth by Controlling Transcriptional Pause Release from Dynamic Enhancers. *Mol Cell*. 2015;60:328-337.
- 24 Zanconato F, Forcato M, Battilana G et al. Genome-wide association between YAP/TAZ/TEAD and AP-1 at enhancers drives oncogenic growth. *Nat Cell Biol*. 2015;17:1218-1227.
- 25 Tremblay AM, Missaglia E, Galli GG et al. The Hippo transducer YAP1 transforms activated satellite cells and is a potent effector of embryonal rhabdomyosarcoma formation. *Cancer Cell*. 2014;26:273-287.
- 26 Kim M, Kim T, Johnson RL et al. Transcriptional co-repressor function of the hippo pathway transducers YAP and TAZ. *Cell reports*. 2015;11:270-282.
- 27 Relaix F, Zammit PS. Satellite cells are essential for skeletal muscle regeneration: the cell on the edge returns centre stage. *Development*. 2012;139:2845-2856.
- 28 Watt KI, Judson R, Medlow P et al. Yap is a novel regulator of C2C12 myogenesis. *Biochem Biophys Res Commun*. 2010;393:619-624.
- 29 Judson RN, Tremblay AM, Knopp P et al. The Hippo pathway member Yap plays a key role in influencing fate decisions in muscle satellite cells. *J Cell Sci*. 2012;125:6009-6019.
- 30 Judson RN, Gray SR, Walker C et al. Constitutive expression of Yes-associated protein (Yap) in adult skeletal muscle fibres induces muscle atrophy and myopathy. *PLoS one*. 2013;8:e59622.
- 31 Watt KI, Turner BJ, Hagg A et al. The Hippo pathway effector YAP is a critical regulator of skeletal muscle fibre size. *Nat Commun*. 2015;6:6048.
- 32 Goodman CA, Dietz JM, Jacobs BL et al. Yes-Associated Protein is up-regulated by mechanical overload and is sufficient to induce skeletal muscle hypertrophy. *FEBS Lett*. 2015;589:1491-1497.
- 33 Morin-Kensicki EM, Boone BN, Howell M et al. Defects in yolk sac vasculogenesis, chorioallantoic fusion, and embryonic axis elongation in mice with targeted disruption of Yap65. *Mol Cell Biol*. 2006;26:77-87.
- 34 Hossain Z, Ali SM, Ko HL et al. Glomerulocystic kidney disease in mice with a targeted inactivation of Wwtr1. *Proc Natl Acad Sci U S A*. 2007;104:1631-1636.
- 35 Park GH, Jeong H, Jeong MG et al. Novel TAZ modulators enhance myogenic differentiation and muscle regeneration. *Br J Pharmacol*. 2014;171:4051-4061.
- 36 Jeon YH, Park YH, Lee JH et al. Selenoprotein W enhances skeletal muscle differentiation by inhibiting TAZ binding to 14-3-3 protein. *Biochim Biophys Acta*. 2014;1843:1356-1364.
- 37 Jeong H, Bae S, An SY et al. TAZ as a novel enhancer of MyoD-mediated myogenic differentiation. *FASEB J*. 2010;24:3310-3320.
- 38 Mohamed A, Sun C, De Mello V et al. The Hippo effector TAZ (WWTR1) transforms myoblasts and TAZ abundance is associated with reduced survival in embryonal rhabdomyosarcoma. *J Pathol*. 2016;240:3-14.
- 39 Schlegelmilch K, Mohseni M, Kirak O et al. Yap1 acts downstream of alpha-catenin to control epidermal proliferation. *Cell*. 2011;144:782-795.
- 40 Tian Y, Kolb R, Hong JH et al. TAZ promotes PC2 degradation through a SCFbeta-Trcp E3 ligase complex. *Mol Cell Biol*. 2007;27:6383-6395.
- 41 Moyle LA, Zammit PS. Isolation, culture and immunostaining of skeletal muscle fibres to study myogenic progression in satellite cells. *Methods Mol Biol*. 2014;1210:63-78.
- 42 Zammit PS, Relaix F, Nagata Y et al. Pax7 and myogenic progression in skeletal muscle satellite cells. *J Cell Sci*. 2006;119:1824-1832.
- 43 Figeac N, Serralbo O, Marcelle C et al. Erbb3 binding protein-1 (Ebp1) controls proliferation and myogenic differentiation of muscle stem cells. *Dev Biol*. 2014;386:135-151.
- 44 Ortuste Quiroga HP, Goto K, Zammit PS. Isolation, Cryosection and Immunostaining of Skeletal Muscle. *Methods Mol Biol*. 2016;1460:85-100.
- 45 Turriziani B, Garcia-Munoz A, Pilkington R et al. On-beads digestion in conjunction with data-dependent mass spectrometry: a shortcut to quantitative and dynamic interaction proteomics. *Biology (Basel)*. 2014;3:320-332.
- 46 Vizcaino JA, Csordas A, Del-Toro N et al. 2016 update of the PRIDE database and its related tools. *Nucleic Acids Res*. 2016;44:11033.
- 47 Plouffe SW, Meng Z, Lin KC et al. Characterization of Hippo Pathway Components by Gene Inactivation. *Mol Cell*. 2016;64:993-1008.
- 48 Park HW, Kim YC, Yu B et al. Alternative Wnt Signaling Activates YAP/TAZ. *Cell*. 2015;162:780-794.
- 49 Holbourn KP, Acharya KR, Perbal B. The CCN family of proteins: structure-function relationships. *Trends in biochemistry sciences*. 2008;33:461-473.
- 50 Mege RM, Goudou D, Diaz C et al. N-cadherin and N-CAM in myoblast fusion: compared localisation and effect of blockade by peptides and antibodies. *J Cell Sci*. 1992;103 (Pt 4):897-906.
- 51 Pallafacchina G, Francois S, Regnault B et al. An adult tissue-specific stem cell in its niche: a gene profiling analysis of in vivo quiescent and activated muscle satellite cells. *Stem Cell Res*. 2010;4:77-91.
- 52 Tremblay AM, Camargo FD. Hippo signaling in mammalian stem cells. *Semin Cell Dev Biol*. 2012;23:818-826.
- 53 Wang W, Li X, Huang J et al. Defining the protein-protein interaction network of the human hippo pathway. *Mol Cell Proteomics*. 2014;13:119-131.
- 54 Price MG, Landsverk ML, Barral JM et al. Two mammalian UNC-45 isoforms are related to distinct cytoskeletal and muscle-specific functions. *J Cell Sci*. 2002;115:4013-4023.
- 55 Cottle DL, McGrath MJ, Cowling BS et al. FHL3 binds MyoD and negatively regulates myotube formation. *J Cell Sci*. 2007;120:1423-1435.
- 56 Benhaddou A, Keime C, Ye T et al. Transcription factor TEAD4 regulates expression of myogenin and the unfolded protein response genes during C2C12 cell differentiation. *Cell Death Differ*. 2012;19:220-231.
- 57 Goetsch SC, Martin CM, Embree LJ et al. Myogenic progenitor cells express filamin C in developing and regenerating skeletal muscle. *Stem Cells Dev*. 2005;14:181-187.
- 58 Millay DP, Sutherland LB, Bassel-Duby R et al. Myomaker is essential for muscle regeneration. *Genes Dev*. 2014;28:1641-1646.
- 59 Ciciliot S, Schiaffino S. Regeneration of mammalian skeletal muscle. Basic mechanisms and clinical implications. *Current pharmaceutical design*. 2010;16:906-914.
- 60 Yu FX, Zhao B, Guan KL. Hippo Pathway in Organ Size Control, Tissue Homeostasis, and Cancer. *Cell*. 2015;163:811-828.
- 61 Hong JH, Hwang ES, McManus MT et al. TAZ, a transcriptional modulator of mesenchymal stem cell differentiation. *Science*. 2005;309:1074-1078.
- 62 Murakami M, Nakagawa M, Olson EN et al. A WW domain protein TAZ is a critical coactivator for TBX5, a transcription factor implicated in Holt-Oram syndrome. *Proc Natl Acad Sci U S A*. 2005;102:18034-18039.

63 Kim J, Jo H, Hong H et al. Actin remodeling factors control ciliogenesis by regulating YAP/TAZ activity and vesicle trafficking. *Nat Commun.* 2015;6:6781.

64 Cai J, Zhang N, Zheng Y et al. The Hippo signaling pathway restricts the oncogenic potential of an intestinal regeneration program. *Genes Dev.* 2010;24:2383-2388.

65 Lee MJ, Ran Byun M, Furutani-Seiki M et al. YAP and TAZ regulate skin wound healing. *J Invest Dermatol.* 2014;134:518-525.

66 Imajo M, Ebisuya M, Nishida E. Dual role of YAP and TAZ in renewal of the intestinal epithelium. *Nat Cell Biol.* 2015;17:7-19.

67 Ulbricht A, Eppler FJ, Tapia VE et al. Cellular mechanotransduction relies on tension-induced and chaperone-assisted autophagy. *Curr Biol.* 2013;23:430-435.

68 Sudol M, Bork P, Einbond A et al. Characterization of the mammalian YAP (Yes-associated protein) gene and its role in defin-

ing a novel protein module, the WW domain. *J Biol Chem.* 1995;270:14733-14741.

69 Kawakami K, Sato S, Ozaki H et al. Six family genes--structure and function as transcription factors and their roles in development. *Bioessays.* 2000;22:616-626.

70 Liu Y, Chakroun I, Yang D et al. Six1 regulates MyoD expression in adult muscle progenitor cells. *PloS one.* 2013;8:e67762.

71 Griffin CA, Kafadar KA, Pavlath GK. MOR23 promotes muscle regeneration and regulates cell adhesion and migration. *Dev Cell.* 2009;17:649-661.

72 Arndt V, Dick N, Tawo R et al. Chaperone-assisted selective autophagy is essential for muscle maintenance. *Curr Biol.* 2010;20:143-148.

73 Moorwood C. Syncoilin, an intermediate filament-like protein linked to the dystrophin associated protein complex in skeletal muscle. *Cell Mol Life Sci.* 2008;65:2957-2963.

74 Bentzinger CF, von Maltzahn J, Dumont NA et al. Wnt7a stimulates myogenic stem cell motility and engraftment resulting in improved muscle strength. *J Cell Biol.* 2014;205:97-111.

75 von Maltzahn J, Chang NC, Bentzinger CF et al. Wnt signaling in myogenesis. *Trends Cell Biol.* 2012;22:602-609.

76 Rudnicki MA, Williams BO. Wnt signaling in bone and muscle. *Bone.* 2015;80:60-66.

77 Takata H, Terada K, Oka H et al. Involvement of Wnt4 signaling during myogenic proliferation and differentiation of skeletal muscle. *Dev Dyn.* 2007;236:2800-2807.

78 Ono Y, Calhabeu F, Morgan JE et al. BMP signalling permits population expansion by preventing premature myogenic differentiation in muscle satellite cells. *Cell death and differentiation.* 2011;18:222-234.



See www.StemCells.com for supporting information available online. STEM CELLS; 00:000-000

Figure 1: Taz levels increase during skeletal muscle regeneration and myogenic differentiation

(A) Yap and Taz mRNA expression in regenerating Tibialis anterior muscle collected at 1, 3, 5, 7 and 14 days post injury. Expression is fold change compared to control undamaged Tibialis anterior (n=3). (B) Yap and Taz mRNA levels in C2C12 myoblasts at 24 h and 48 h in proliferation medium, and 24 h, 48 h, 72 h and 96 h in differentiation medium, expressed as fold change compared to 24 h proliferation time-point (n=3). (C) Representative Western blots from biological replicate 4 (n=4) showing total Yap, Taz, and phosphorylated Yap and Taz levels in C2C12 myoblasts at 24 h and 48 h in proliferation medium, and 24 h, 48 h, 72 h and 96 h in differentiation medium, with relevant α -Tubulin or Gapdh loading controls. (D) Taz mRNA increased through differentiation in plated satellite cell-derived myoblasts at 12 h, 24 h, 48 h. Data is mean \pm SEM from 3 experiments where an asterisk denotes significant difference ($p<0.05$) from 0 h using an unpaired Student's *t* test. (E) C2C12 proliferating myoblasts co-immunolabelled for Yap and Taz. (F) Plated satellite cell-derived myoblasts co-immunolabelled with MyoD and Taz after 36 hrs ex-vivo. (G) Plated satellite cell-derived myotubes co-immunolabelled with myogenin and Taz after 48 hrs ex vivo. (H) Confocal images of satellite cells co-immunolabelled with MyoD and Taz on isolated fibres cultured ex vivo for 72 h; arrow points to Taz-containing nuclei. Scale bar equals 100 μ m (F-G).

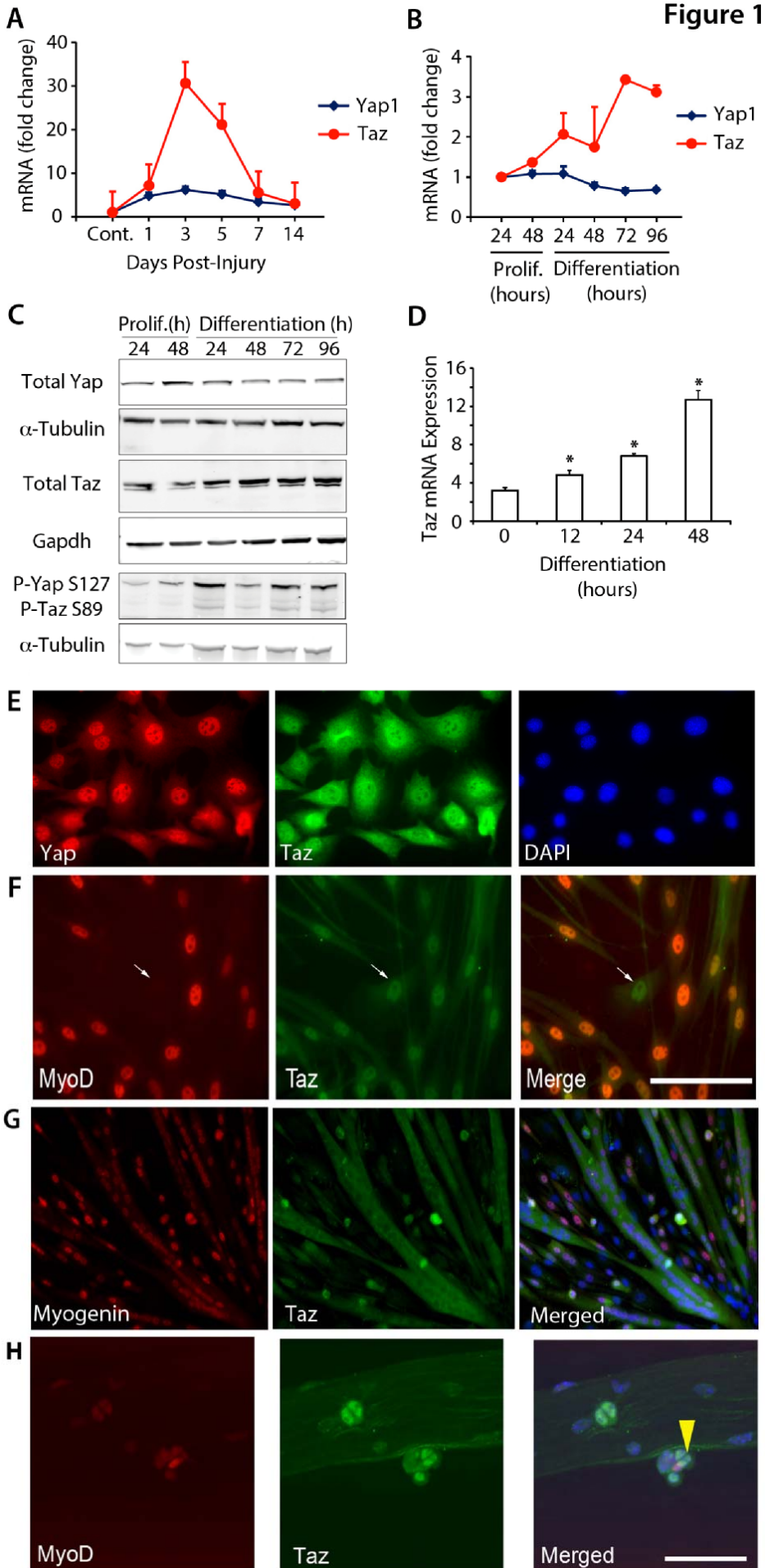


Figure 2. Taz controls satellite cell-derived myoblast proliferation

(A) Representative images of EdU incorporation in satellite cell-derived myoblasts 48 h following transduction with Control Vector (RV), or retroviral constructs encoding wildtype human TAZ or constitutively active TAZ S89A, where GFP marks transduced cells. (B) Quantification of GFP+ cells with EdU incorporation shows that TAZ or TAZ S89A significantly increases EdU incorporation, and so proliferation rate (n=5 mice). (C) Representative images of EdU incorporation in satellite cell-derived myoblasts following *Yap* and/or *Taz* knockdown using siControl, siYap, siTaz or siYap+Taz transfection. (D) Quantification of EdU incorporation shows that knockdown of Yap, Taz or both Yap and Taz reduces the proliferation rate (n=5 mice). (E) Relative gene expression measured by RT-qPCR in satellite cell-derived myoblasts compared to si Control under proliferation conditions following siControl, siYap, siTaz or siYap+Taz knockdown, normalized to Gapdh (n=5 mice except for MyHC/MyoD where n=3). Data presented as mean±SEM where an asterisk denotes significant difference from control retrovirus/control siRNA ($p<0.05$) using Student's *t* test. Scale bar equals 100 μ m.

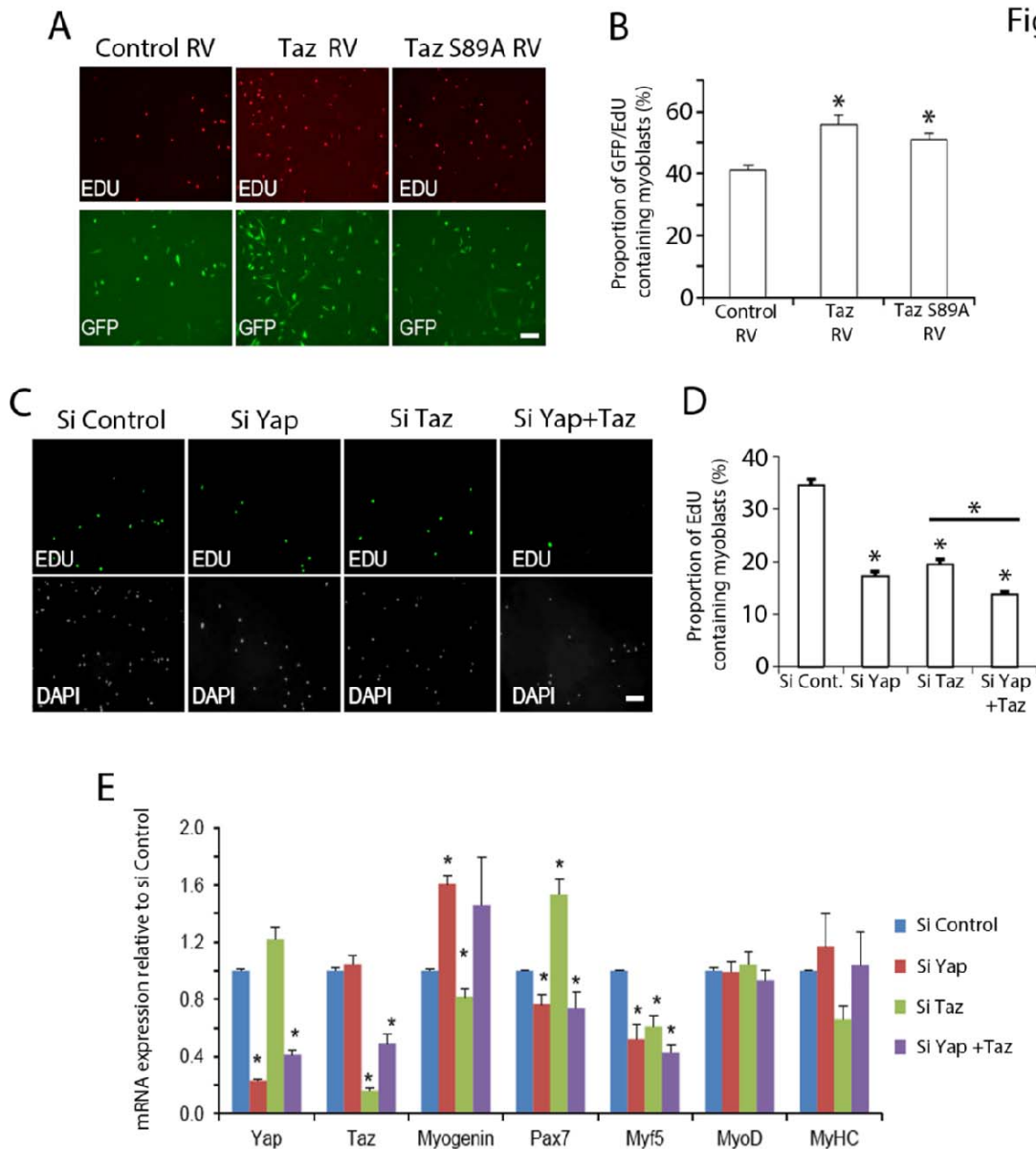


Figure 3: Taz regulates fusion of satellite cell-derived myoblasts

(A and B) Satellite cells on isolated myofibres were transduced with retroviruses encoding wildtype human TAZ, constitutively active TAZ S89A or Control vector, and cultured *ex vivo* for 72 h, before being co-immunolabelled for eGFP and Pax7, or eGFP and Myogenin. Quantification of the proportion of (A) GFP/Pax7 and (B) GFP/myogenin satellite cells in the *ex vivo* cultures after 72 h (n=3 mice). (C and D) Quantification of the proportion of expanded plated satellite cell-derived myoblasts transduced with control retroviral vector, wildtype human TAZ or TAZ S89A and incubated in differentiation medium for 24 h before being co-immunolabelled as myocytes for eGFP/Pax7 or eGFP/myogenin, illustrated in (E) (n=4 mice). (F) Representative images of expanded plated satellite cell-derived myoblasts transduced with wildtype human TAZ, TAZ S89A or Control vector and incubated in differentiation medium before being co-immunolabelled for eGFP/Myosin Heavy Chain (MyHC). (G) Quantification of the proportion of nuclei within GFP/MyHC myotubes shows that TAZ or TAZ S89A increases myogenic fusion (n=5 mice). (H) Representative images of satellite cell-derived myoblasts transfected with siRNA control or siRNA Taz and immunolabelled for MyHC after 24 h. (I) Quantification shows a trend towards reduced fusion ($p=0.06$) with siRNA Taz (n=3 mice). (J) Representative images of myotubes formed from satellite cell-derived myoblasts isolated from wildtype (*Wwtr1*^{+/+}) or Taz (*Wwtr1*^{-/-}) knockout mice after 24 h in differentiation medium. (K) Quantification reveals less fusion in the Taz (*Wwtr1*^{-/-}) knockout mice compared to controls (n=4 per genotype). Data is mean±SEM where an asterisk denotes significant difference ($p<0.05$) using a Student's *t* test from control vector/control siRNA/*Wwtr1*^{+/+} as appropriate. Scale bars equals 100µm.

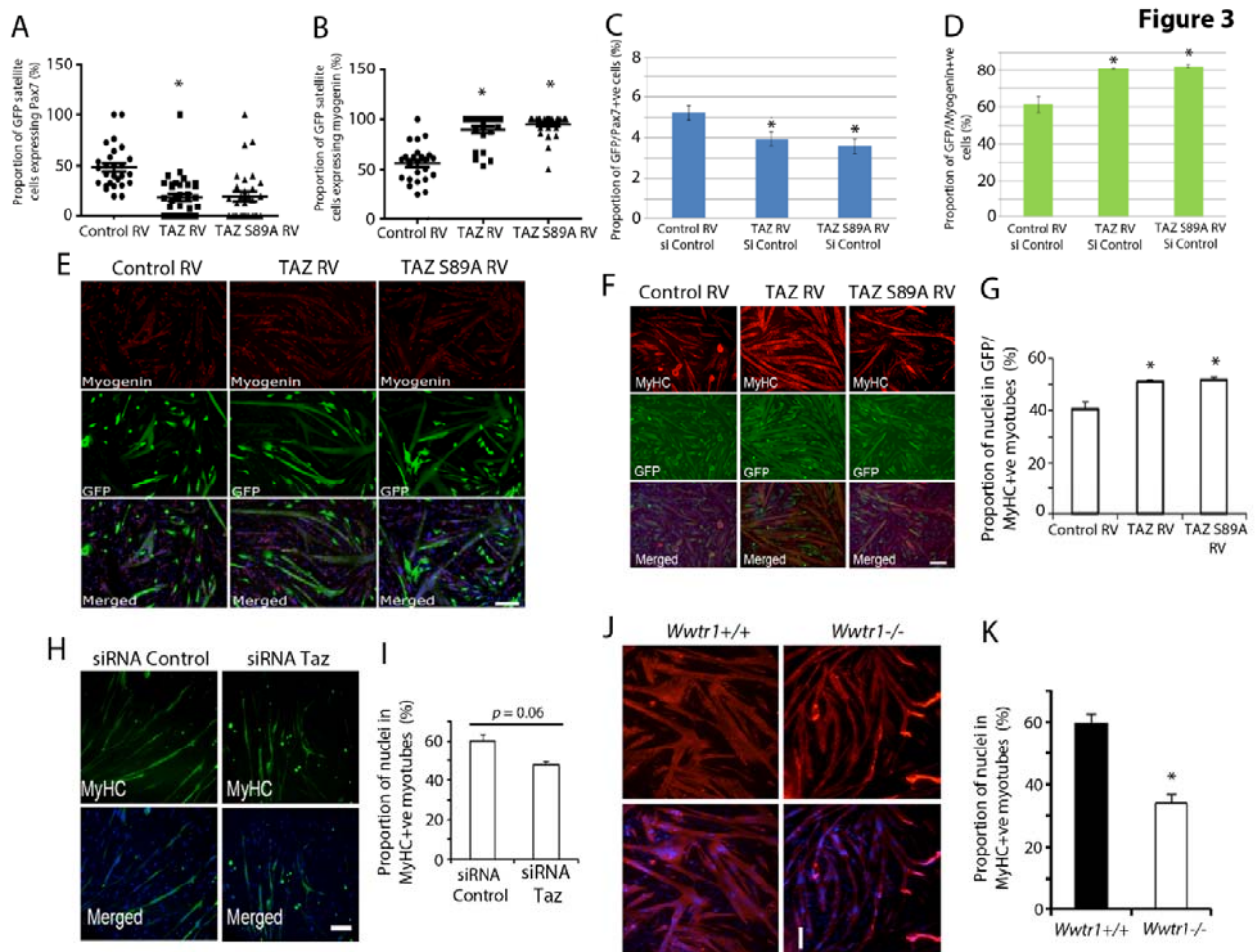


Figure 4. Characterization of skeletal muscle and muscle regeneration in Taz (*Wwtr1*^{-/-}) knockout mice

(A) Body weight of 6-week old Taz (*Wwtr1*^{-/-}) knockout (Taz KO) mice (n=7) compared to wildtype *Wwtr1*^{+/+} control (WT) (n=9). **(B-E)** Quantification of muscle weight of TA, Soleus, EDL and Gastrocnemius from WT and Taz KO mice (n=3 mice). **(F)** Satellite cell and **(G)** myonuclei number per myofiber isolated from the EDL of WT or Taz KO mice (n=4 mice of each genotype). **(H)** Representative images of soleus from 6-week-old WT and Taz KO after ATPase histochemical staining at pH4.47 to show slow type I (dark) and fast type IIa (light/no stain) muscle fibre types. **(I)** Quantification showing less total myofibres in the soleus of Taz KO mice, with numbers of both type I and type IIa reduced (n=3 mice of each genotype). **(J)** Quantification of cross section area (CSA) of type I and type IIa reveals that myofibres from Taz KO are unchanged compared to controls (n=3 mice per genotype). **(K)** Representative images and **(L)** quantification of the proportion of the neonatal MyHC area of regenerating tibialis anterior myofibres co-immunolabelled for neonatal MyHC (NeoMyHC)/laminin at 5 days post injury (dpi) with cardiotoxin (n=4 mice of each genotype). **(M)** Representative images of H&E staining at 10 dpi of TA from Taz KO and WT mice. **(N)** Quantification of the number of myofibres with a central nucleus per field of 10 dpi TA (n=3 mice per genotype). Data is mean±SEM where an asterisk denotes significant difference ($p < 0.05$) between WT and Taz KO using a Student's *t* test. Scale bar equals 100 μ m.

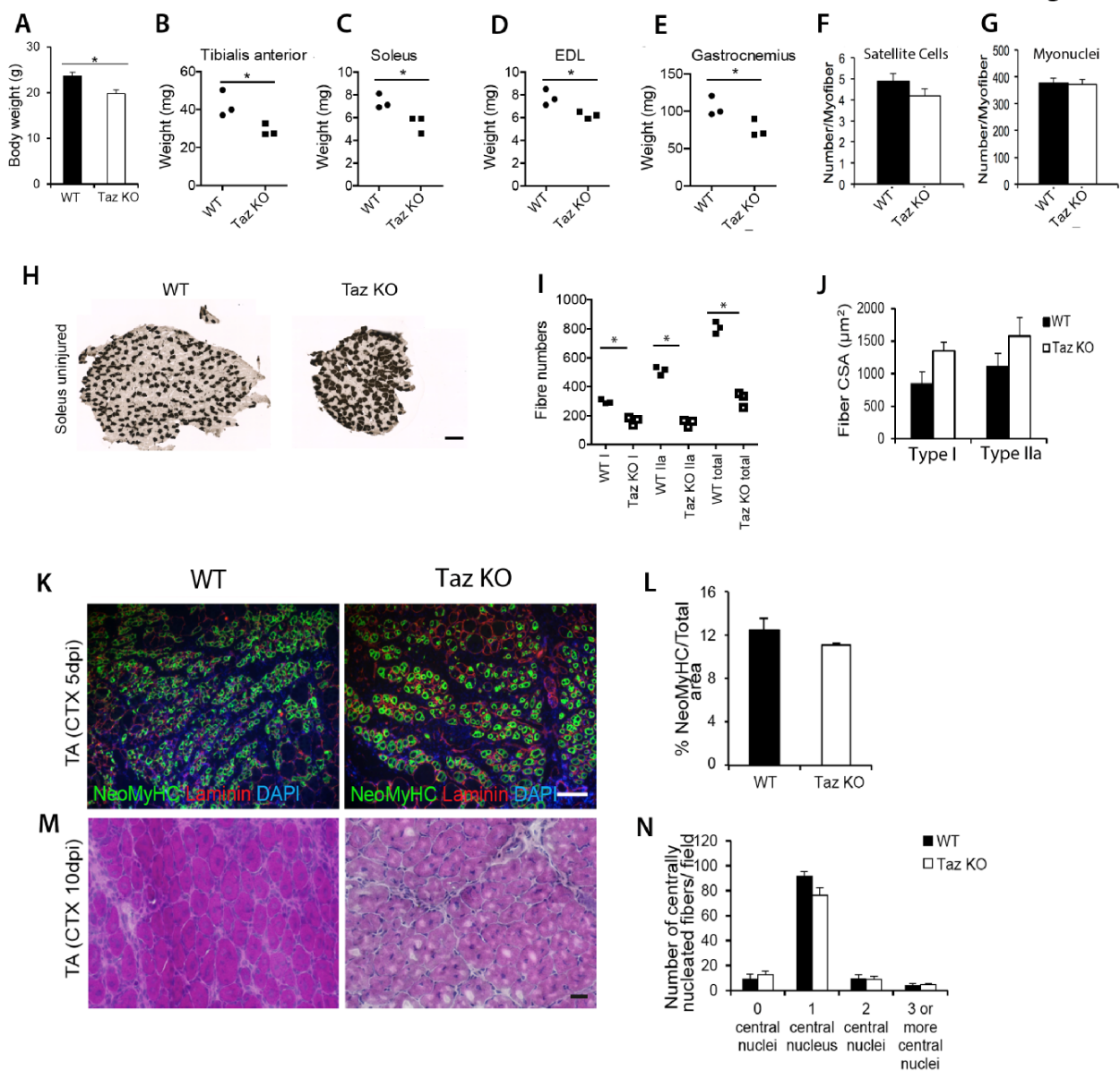
Figure 4

Figure 5. Yap conditional knockout in satellite cells affects muscle regeneration

(A) Time course for analysis of Yap conditional knockout and control mice after tamoxifen administration via intraperitoneal injection (IP) and food, and cardiotoxin-induced injury (CTX). **(B and C)** Representative images and quantification of TA cryosections 5 dpi after CTX injury of *Pax7^{CreERT/+}:Yap^{flx/flx}:Rosa26^{LacZ}* (*Pax7Cre Yapfl/fl*) and control *Pax7^{CreERT/+}:Yap^{flx/+}:Rosa26^{LacZ}* (*Pax7Cre Yapfl/+*) mice, co-immunolabelled for neonatal MyHC (NeoMyHC)/laminin to identify regenerating myofibres (n=4 mice per genotype). **(D - F)** Representative images and quantification of cryosections of TA muscles after 5 or 10 dpi, immunolabelled for Pax7 to label satellite cells (5 dpi: n=4 per genotype; 10 dpi: n=4 *Pax7Cre Yapfl/fl* and n=3 *Pax7Cre Yapfl/+*). **(G)** Representative images of H&E staining and **(H)** quantification of centrally nucleated myofibre number per field of 10 dpi TA. Data is mean±SEM where an asterisk denotes significant difference ($p < 0.05$) between *Pax7Cre Yapfl/+* and *Pax7Cre Yapfl/fl* using a Student's *t* test. Scale bar equals 100 μ m.

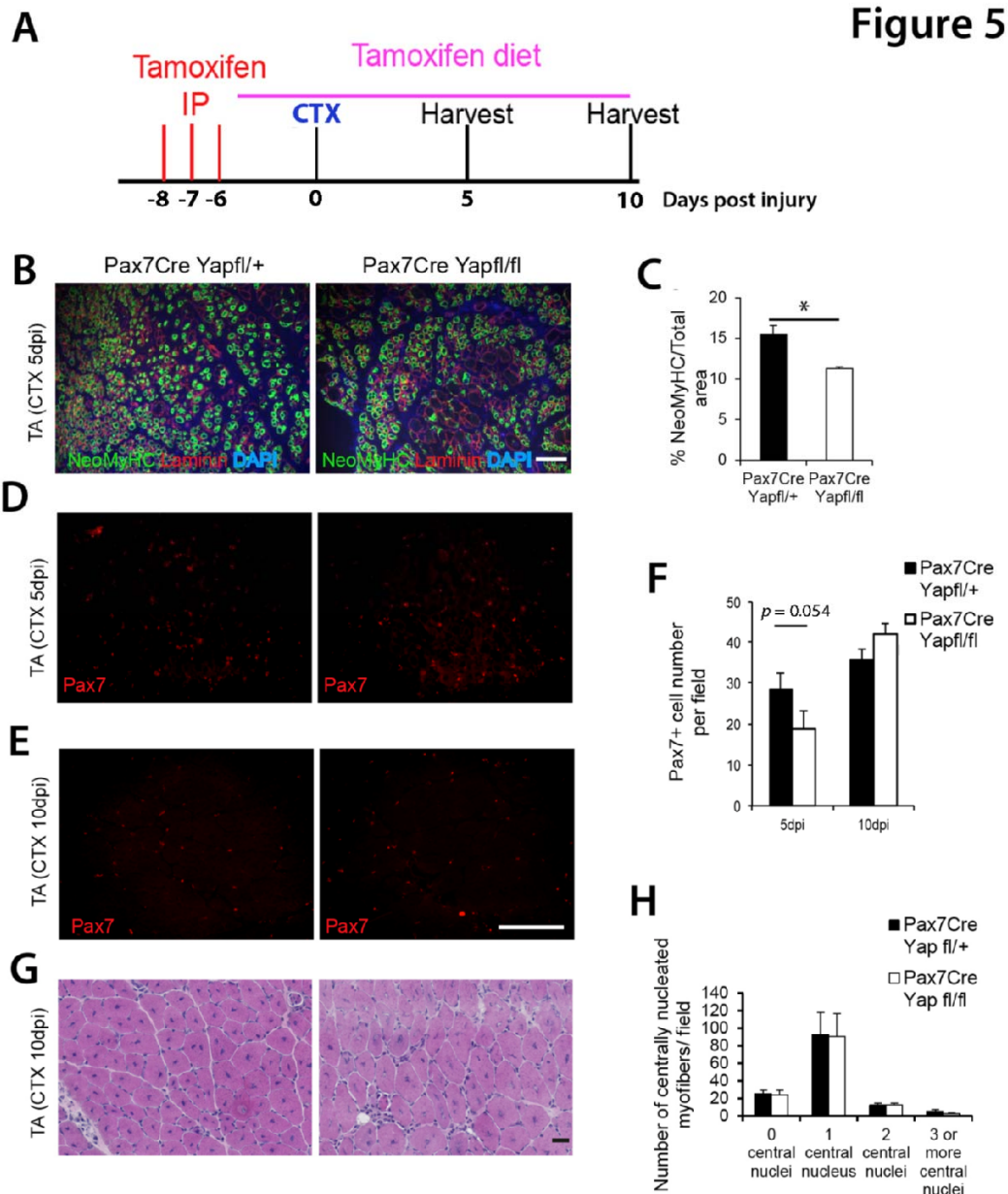
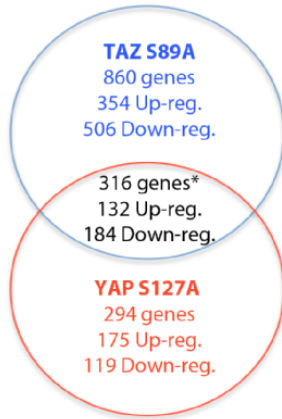


Figure 6: Genes regulated by TAZ S89A or YAP S127A and proteins bound by TAZ and/or YAP

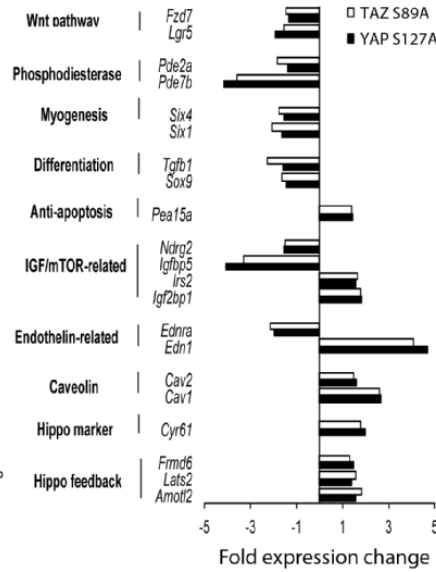
(A) Venn diagram displaying the number of genes modulated by TAZ S89A and/or YAP S127A versus control retrovirus (up-reg: up-regulated; down-reg: down-regulated) at either 24 or 48 hours. **(B)** Expression fold change for genes that were regulated by both TAZ S89A and YAP S127A in transduced satellite cell-derived myoblasts versus control retrovirus at either 24 or 48 hours. **(C)** Expression fold change for genes that were regulated only by TAZ S89A at either 24 or 48 hours. **(D)** All TAZ and/or YAP interacting proteins identified by mass spectrometry in C2C12 myoblasts and myotubes. Those previously identified are in red [53] and novel proteins in black, with those of particular interest in blue. To minimise false positives, selected cut-off values were a ratio of ≥ 2 compared to empty vector and $p < 0.05$ Student's *t*-test between each dataset and control vector.

A

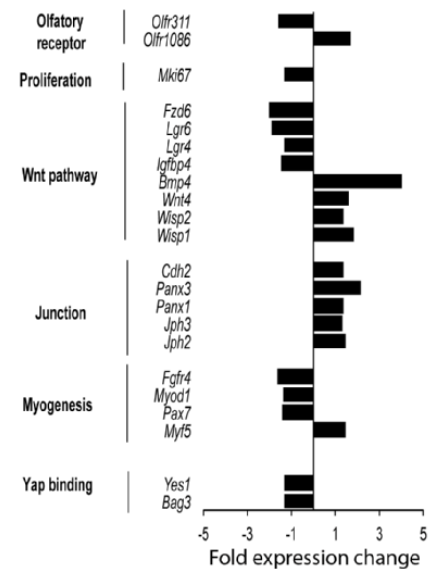


* 3 genes induced by TAZ but repressed by YAP
* 1 gene induced by YAP but repressed by TAZ

B TAZ and YAP regulated genes



C TAZ regulated genes

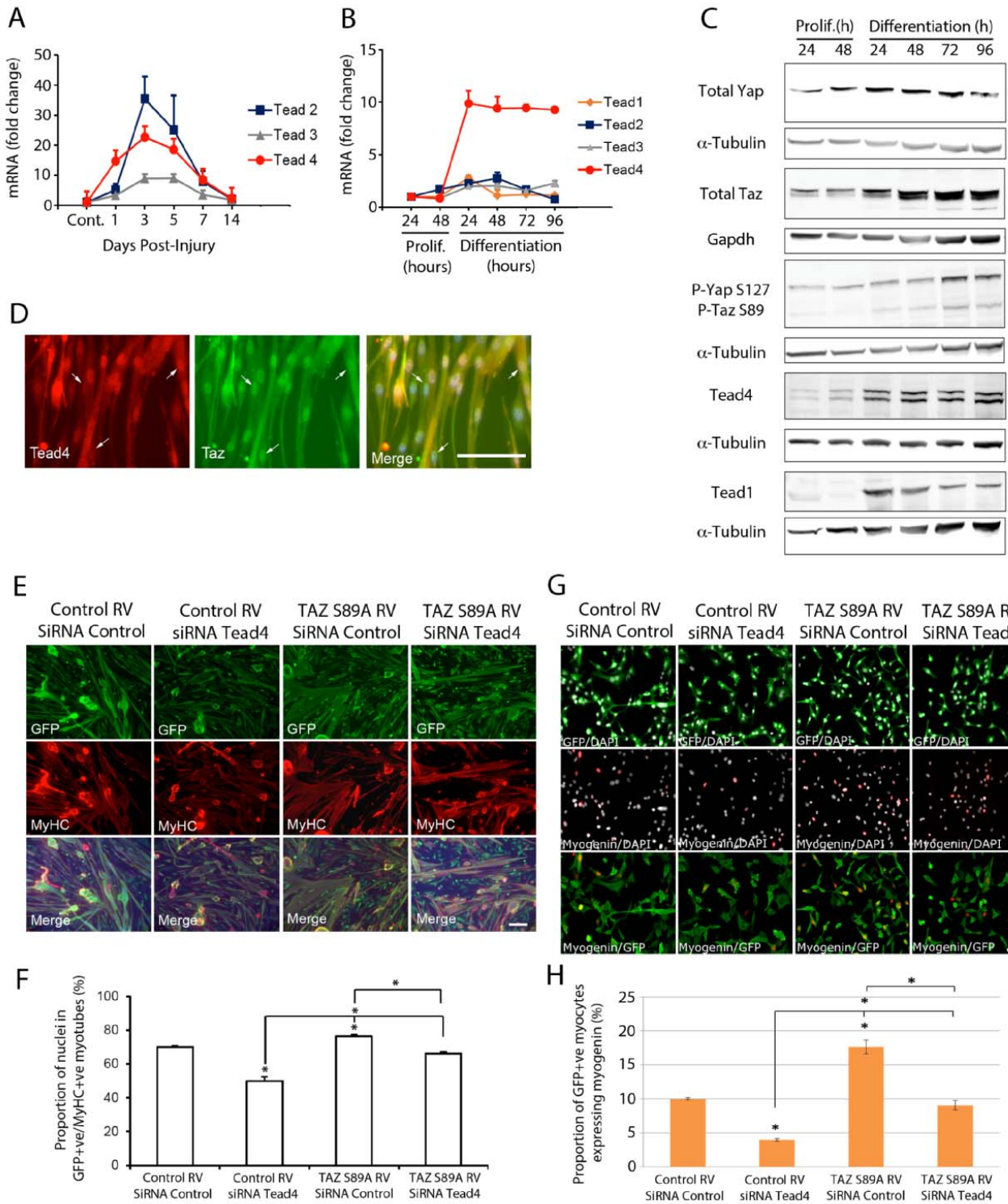


D

	Myoblast and Myotube	Myoblast only	Myotube only
YAP and TAZ	Amot, Amotl1, Lin7c, Mpdz, Mpp5, Tead1, Tead2, Ywhab, Ywhae, Ywhag, Ywhah, Ywhaz	Ahdcl, Arpc5, Cenpc, Hira, Lemd2, Nf2, Nol11, Rassf8, Strn3, Tead4, Trp53bp2, Trrap	Adam34, Arpc5l, Bag2, Bag3, Cnot3, Crip2, Eppk1, Fhl1, Fxr2, Gatad2a, Golgb1, Grwd1, Hspe1, Lasp1, Limd2, Mif, Nefm, Nes, Pa2g4, Rps21, Rpsa, Sars, Slc2a1, Slu7, Sync, Tpm1
TAZ only	Myh1, Plec, Uqcrh, Taz	Ablim1, Adnp, Akap8, Amotl2, Aurkb, Banf1, Baz1b, Btrc, Cd44, Chaf1a, Chchd6, Chd4, Ctbp2, Dclk1, Ddx27, Dlg3, Dst, Erh, Fbxw11, Flot1, Fytd1, Gpx8, Hat1, Hp1bp3, Hspa1a, Ifi214, Kdm1a, Las1l, Lgals3, Lysmd2, Mbnl2, Mdn1, Murc, Ncoa5, Ndc1, Nhp2, Nkap, Nup153, Nup51, Nup88, Pard3, Pelp1, Pml, Polr1a, Ppp1r11, Prdx6, Rae1, Rai1, Runx1, Sarnp, Sf3a3, Sf3b6, Sfn, Slc25a11, Smarcc2, Snrpa1, Son, Spen, Sympk, Syne3, Taf15, Taf9, Tead3, Thrap3, Timm44, Top2b, Tuba4a, Wdr74, Ywhaq	Aatf, Casq1, Ckb, Coro6, Fhl3, Hspb8, Lrrfp2, Myh2, Myl1, Myom2, Nefl, Pgm5, Prcc2b, Rap1gds1, Sntb1, Sorbs1, Ttll12, Ttn, Unc45a, Usp15
YAP only	Amotl2, Dst, Ehd2, Hspa1a, Sfn, Yap1, Ywhaq	Ahrr, Chd3, Hspa5, Hspa8, Ktn1, Nfya, Rassf8, Sqstm1, Stk11, Urb1, Vdac1	11/19/2112, Acsl4, Actb, Angptl2, Asna1, Atad5, Atxn11, Bax, Dynll2, Dynll1, Btf3, Ccdc112a, Cdc42bbp, Cep171, Chaf1b, Chmp5, Cnn2, Col18a1, Ctnb2, D8Ert738e, Dbnl, Decr1, Dlg1, Dpysl3, Dvl2, Dvl3, Eif4e, Etf1, Fam114a1, Fam114a2, Fam195b, Fbln2, Filip1l, Gnao1, Gnb2, Gnb4, Hectd1, Hist1h2bb, Hist1h2ba, Hist3h2ba, Hist3h2bb, Hk2, Hk1, Hspa4l, Hspb1, Htra1, Iffo1, Igf2bp2, Igf2bp3, Jcad, Lar4, Ldb3, Lgals1, Lmo7, Lmod1, Lonp1, Lox, Lpp, Mapre1, Mecr, Mgea5, Mthfd1, Mtpn, Myo1c, Myo5a, Myo6, Ndrq1, Nup85, Akap2, Pck2, Pcd6, Pdlim1, Pdlim2, Pdlim5, Pkm, Plec, Plekhg5, Prdx4, Prdx5, Prkaa1, Psmg1, Ptrf, Rab11, Ranbp1, Rps28, Sec61b, Sh3gl1, Sh3gl2, Sipa1, Slc4a1ap, Smarca4, Srp54, Srprb, Stk3, Stub1, Tbl2, Tead3, Tes, Tjp1, Tnni2, Tpm3, Tpm4, Tsr1, Tuba1a, Tuba3a, Tuba1b, Txlna, Ubqln1, Uqcrh, Utrn, Vasp, Wasf2, Wiz, Zranb2

Figure 7: TAZ operates through Tead4 to control myogenic differentiation

(A) Tead2-4 mRNA expression in regenerating tibialis anterior muscle collected at 1, 3, 5, 7 and 14 days post injury with cardiotoxin. Expression is presented as fold change compared to control undamaged TA (n=3). **(B)** Tead1-4 mRNA levels in C2C12 myoblasts at 24 h and 48 h in proliferation medium, and 24 h, 48 h, 72 h and 96 h in differentiation medium, expressed as fold change compared to 24 h proliferation time-point (n=3). **(C)** Representative Western blots of C2C12 myoblast lysate collected at 24 h and 48 h in proliferation medium and 24 h, 48 h, 72 h and 96 h in differentiation medium and immunoblotted for Yap, Taz, Tead1 (biological replicate 3), phosphorylated Yap and Taz (biological replicate 2) and Tead4 (biological replicate 1) (n=4), with relevant α -Tubulin or Gapdh loading controls. **(D)** Representative images of plated satellite cell-derived myoblasts co-immunolabelled with Tead4 and Taz cultured under differentiation conditions for 24 h. **(E)** Representative images of co-immunolabelling of myotubes formed from satellite cell-derived myoblasts following TAZ S89A or control vector transduction and/or siRNA knockdown of Tead4 or siRNA control. GFP labels transduced cells and MyHC identifies myotubes. **(F)** Comparison of the proportion of nuclei in GFP+ve/MyHC+ve myotubes under each condition shows that TAZ requires Tead4 to enhance differentiation (n=3 mice). **(G)** Representative images of co-immunolabelling of myocytes formed from satellite cell-derived myoblasts following TAZ S89A or control vector transduction and/or siRNA knockdown of Tead4 or siRNA control, and 24 h in differentiation medium. GFP labels transduced cells and Myogenin identifies myocytes. **(H)** Comparison of the proportion of GFP+ve/Myogenin+ve myocytes under each condition shows that TAZ-induced myogenic differentiation operates through Tead4 (n=3 mice). Data is mean \pm SEM from 3 mice, where an asterisk denotes significant difference ($p<0.05$) from Control Vector/siRNA Control, or as indicated by bars, using a paired Student's *t* test. Scale bar equals 100 μ m.



Graphical Abstract: In skeletal muscle, Taz and Yap both enhance satellite cell derived-myoblast proliferation, but during the later stages of myogenesis, Taz switches to influence satellite cell fate by promoting myogenic differentiation over self-renewal.

